Angewandte Chemie
Eine Zeitschrift der Gesellschaft Deutscher Chemiker

Supporting Information

German Edition: DOI:

The Mechanism of Color Change in the Neon Tetra Fish: a Light-Induced Tunable Photonic Crystal Array**

*Dvir Gur, Benjamin A. Palmer, Ben Leshem, Dan Oron, Peter Fratzl, Steve Weiner, and Lia Addadi**

anie_201502268_sm_miscellaneous_information.pdf
anie_201502268_sm_S1.avi
anie_201502268_sm_S2.mp4

Supporting information:

Materials and methods

Fish

Neon tetra fish (*Paracheirodon innesi*) were bought from a local distributor (Peka, Rehovot, Israel) and were maintained in an aquarium.

Reflectance Measurements. Longitudinal sections of the neon tetra lateral stripe ~3× 1 cm^2 in area and ~5mm in thickness were dissected by hand using a scalpel. The reflectance of these sections was measured from 5 different fish after 1 hour of dark adaption. The tissue was kept immersed in physiological buffer (PBS, 136 mOsm/kg) throughout the whole measurement. We used a previously developed custom built microscope for measuring the reflectance, consisting of a microspectrophotometer, two CCD cameras, and a high numerical aperture objective [3]. The custom built microscope enabled us acquiring the reflectance spectrum and image of the epidermal layer of the lateral stripe as well as obtaining the Fourier transform of the reflectance for the same location in the stripe. The reflectance spectrum and the image acquired by the microscope were used to determine the reflectance intensity, which was normalized to the reflectance of a silver mirror and to the coverage area of the crystal stacks beneath the skin. The coverage areas were determined from the light microscope images by integrating all the areas covered with crystal stacks. The Fourier transformation of the images was obtained in order to verify that most of the highly spread reflected light from lateral stripe was indeed collected. For further information, please consult ref 3e.

Cryo-SEM. Sections of the fish lateral stripe ~2× 2 mm^2 in area and 200 μm in thickness were prepared while immersed in a physiological buffer (PBS, 136 mOsm/kg). Fresh sections were sandwiched between two metal discs (3 mm diameter, 0.2 mm cavity and a flat cover), and cryo-immobilized in a high-pressure freezing device (HPM10; Bal-Tec). The frozen samples were carved out from the discs, were mounted in vertical position on a holder under liquid nitrogen and transferred to a freeze fracture device (BAF60; Bal-Tec) using a vacuum cryo-transfer device (VCT 100; Bal-Tec). There the samples were freeze fractured to form a transversal section. Samples were observed in an Ultra 55 SEM (Zeiss) using a secondary electron in-lens detector , maintaining the frozen-hydrated state

with a cryo-stage operating at a temperature of −120 °C. Measurements of crystal thickness and cytoplasm spacings were performed from the cryo-SEM micrographs choosing the crystals that appeared to be edge-on to the fracture surface.

Simulated reflectivity. Prediction of the percent reflectivity at normal incidence can be calculated using the mean measured values and standard deviations for crystal thicknesses and the spacing between them (from cryo-SEM), using a Monte-Carlo calculation, i.e. a repeated random sampling algorithm. Using this approach 500 stochastic realizations of the multilayer stack were defined, where the thickness of each layer was randomly picked from the experimentally measured layer thickness distribution (by cryo-SEM). The spectral reflectivity was then calculated for each realization of the multilayer stack, and the results were averaged. In more detail, for each layer we define the following 2x2 matrix:

(1) $$m_j = \begin{pmatrix} Cos\beta_j & -\frac{i}{n_j} Sin\beta_j \\ -n_j Sin\beta_j & Cos\beta_j \end{pmatrix} \qquad \text{where} \qquad \beta_j = \frac{2\pi}{\lambda} n_j d_j$$

such that d_j is the thickness of the j^{th} layer and n_j its refractive index.
The set of k double layers is characterized by an overall reflectivity 2x2 matrix:

(2) $$M_j = \prod_{j=1}^{j=2k} m_j$$

The reflectivity in each case was then extracted from the following expression:

(3) $$R = \left| \frac{(m_{11} + m_{12}) - (m_{21} + m_{22})}{(m_{11} + m_{12}) + (m_{21} + m_{22})} \right|^2$$

The refractive index of the birefringent guanine crystal was calculated according to impinging angle of incident light based the following expression:

(4)

$$\frac{1}{n^2} = \frac{cos^2\theta}{n^2{}_e} + \frac{sin^2\theta}{n^2{}_0}$$

When: n_e=1.83, n_o=1.45

The refractive index of cytoplasm was taken to be n=1.33 in all cases.

We neglect the weak dependence of the refractive index on the wavelength and assume that all the interfaces are parallel.

Microbeam WAXD measurements.

Longitudinal sections ~ 3× 1 cm^2 in area and ~5mm in thickness, immersed in a physiological buffer (PBS, 136 mOsm/kg) were mounted in a copper frame between 2 kapton windows. In situ WAXD was obtained at the μ-Spot beamline, in the synchrotron radiation facility BESSY II, Helmholtz-Zentrum Berlin für Materialien und Energie, Berlin, Germany. Samples were mounted on a y–z scanning table and one spot loop scans of the sample in areas of interest were performed. The thin sections were placed face on under the X-ray beam in the light-adapted state, WAXS patterns were collected only after the diffraction pattern was stable over ~10min. Lights were switched off and data was collected at 60 second intervals with a measuring time of 3 seconds for up to 2hrs, while performing cycles of light on-off-on. The microbeam was defined by a toroidal mirror and a pinhole of either 10 μm or 30 μm diameter close to the sample, providing a beam size of approximately 10×10μm^2 or 30×30μm^2 at the sample position. An energy of 15keV (λ = 0.82656Å) was selected by a Mo/BC multilayer monochromator. The 2D SAXS/WAXD patterns were measured by using a MarMosaic 225 CCD-based area detector (Rayonix) placed at a sample-detector distance of 286 mm. The beam center in the detector and the sample-detector distance were calibrated using a powder X-ray diffraction pattern of synthetic guanine powder standard (Sigma Aldrich). Radial integration of the 2D scattering patterns was performed by using Fit2D. The data were normalized with respect to the primary beam monitor (ionization chamber) and corrected for background caused by pinhole and air scattering.

Figures:

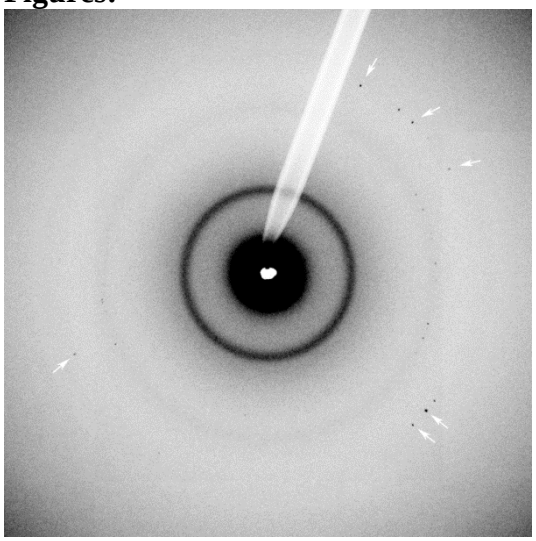

Figure S1. Diffraction pattern taken from the lateral stripe of the neon tetra. Each distinct spot corresponds to a single iridophore. The diffraction points located on the external radius ring corresponds to the (012) plane (arrows).

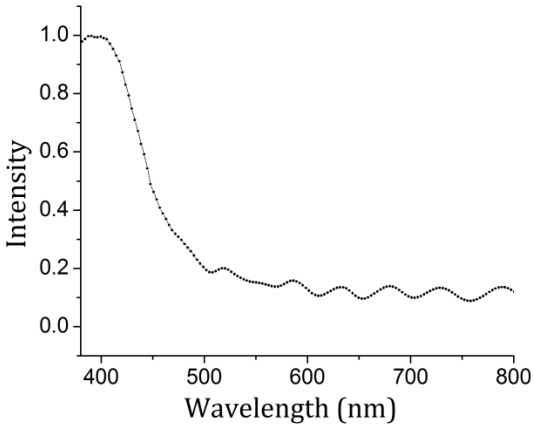

Figure S2. Simulated reflectance spectrum of the dark adapted state. The structural parameters used were derived from the cryo-SEM of the light adapted state, where a shrinkage of the cytoplasm thickness from 155nm to 125nm was taken into account.

Movie S1.A video showing the color change dynamics of the lateral stripe of the neon tetra after 1 hour of dark adaption. Initially the lateral stripe is violet-indigo. Stimulated by the exposure to bright light, it changes colour to blue-green.

Movie S2. A video showing one individual diffraction spot monitored through a full cycle of alternating light stimulations (light-dark-light). Diffraction patterns were acquired every 60 seconds with a total of 115 patterns. The video corresponds to the spectra shown in Figure 5.